1253S

EUROPEAN ORGANIZATION FOR NUCLEAR RESEARCH

SPS DIVISION

SPS/ABT/Tech. Note 88-5

FIRST COMMENTS ON THE INTERACTION OF SYNCHROTON LIGHT WITH THE ELECTROSTATIC SEPTA OF THE SPS

R. Dubois, R.L. Keizer, E. Weisse

Prévessin, April 1988

LIST OF SYMBOLS USED

C_{ae} [pF]	= anode to earth stray capacity
C_{ac} [pF]	= anode to cathode stray capacity
C_{ce} [pF]	= cathode to earth stray capacity
E [GeV]	= positron energy
i [mA]	= circulating positron current
i_{acc} [mA]	= average accelerated intensity
i_{coa} [mA]	= coasting beam intensity
i_s [$\mu A\ GeV^{-1}\ mA^{-1}$]	= specific photo-electric current emitted from the cathode
I [μA]	= photo electron current emitted from the cathode
I_{ai} [μA]	= individual anode currents
I_{gi} [μA]	= individual gap currents
I_{tot} [μA]	= total cathode current
ℓ [m]	= distance between bending magnet and cathode
n_γ [$10^{14}\ s^{-1}\ GeV^{-1}\ mA^{-1}$]	= number of photons received per s per GeV and per mA of circulating beam
$\overline{n_\gamma}$ [$10^{14}\ s^{-1}\ m^{-1}$]	= number of photons emitted per s and per m of beam trajectory
N_{e^+}	= number of circulating positrons
N_{tot} [10^{14}]	= total number of photons received by each cathode during one acceleration cycle
N_γ [s^{-1}]	= number of photons received by surface S per s
Q_{tot} [μc]	= total charge emitted by a particular cathode during one acceleration cycle

r [m]	= distance between cathode and central axis
S	= surface receiving photons
U_{cir} [kV]	= cathode potential
α [mrad]	= incident angle of photons
β [rad]	= angle of photon emission
δ	= coefficient for the emission of photo-electrons
ρ [m]	= radius of curvature of a SPS bending magnet
τ_p [s]	= time constant of the prompt spark rate
τ_r [s]	= time constant of the retarded spark rate

C O N T E N T S

		No. page
1.	INTRODUCTION	1
2.	ESTIMATION OF THE NUMBER OF PHOTONS RECEIVED BY THE CATHODE AND OF THE PHOTO EMISSION CURRENTS	3
3.	PHOTO EMISSION CURRENTS MEASURED	10
	3.1. The HT-circuit	10
	3.2. Photo emission currents at constant cathode potential	12
4.	SPARKING OF THE SEPTA	17
	4.1. Spark time spectra and shutter efficiency	17
	4.2. Spark rate decay time constants of prompt and retarded sparking	19
	4.3. The retracted cathode experiment	23
5.	CONCLUSIONS	26
6.	RECOMMENDATIONS	27
7.	ACKNOWLEDGEMENTS	27

INTRODUCTION.

The first acceleration tests with positrons in the SPS have shown that above a certain energy, roughly 6 GeV, the electrostatic septa set-in to spark at a very high rate.

This behaviour was not entirely unexpected, taking into account the amount of synchroton light hitting the e.s. septa and the resulting photo-electric current between the electrodes. But there remained the question of relating these phenomena to a spark mechanism. It was then decided to build and to equip the first of the five septum units in one extraction channel, LSS6, with a "shutter". Such a device consists of a 3 mm thick tungsten screen which, during the positron cycles, is raised in front of the septum to intercept the synchroton light generated upstream. During the proton cycles, the shutter is lowered to allow the extracted p-beam to pass, see Fig. 1.

This note describes and analyzes the very high spark rates which have been recorded during the machine development runs in September and October 1987. Novel characteristic features such as prompt sparking during the positron cycles and retarded sparking, which occurs throughout the supercycle, are discussed. The shutter is shown to prevent all sparking in the first septum.

A large number of questions concerning these characteristics and the trigger mechanism of sparks remain to be answered. Further studies and experiments are therefore required.

Since the prototype performed efficiently, it was decided to build more shutters and to equip more septum units in the two extraction channels LSS2 and LSS6 during the 87/88 winter shutdown.

The results mentioned in this note bear partly on the question whether the 300 kV dc power supplies used for the septa should be pulsed instead of using a system of mobile shutters.

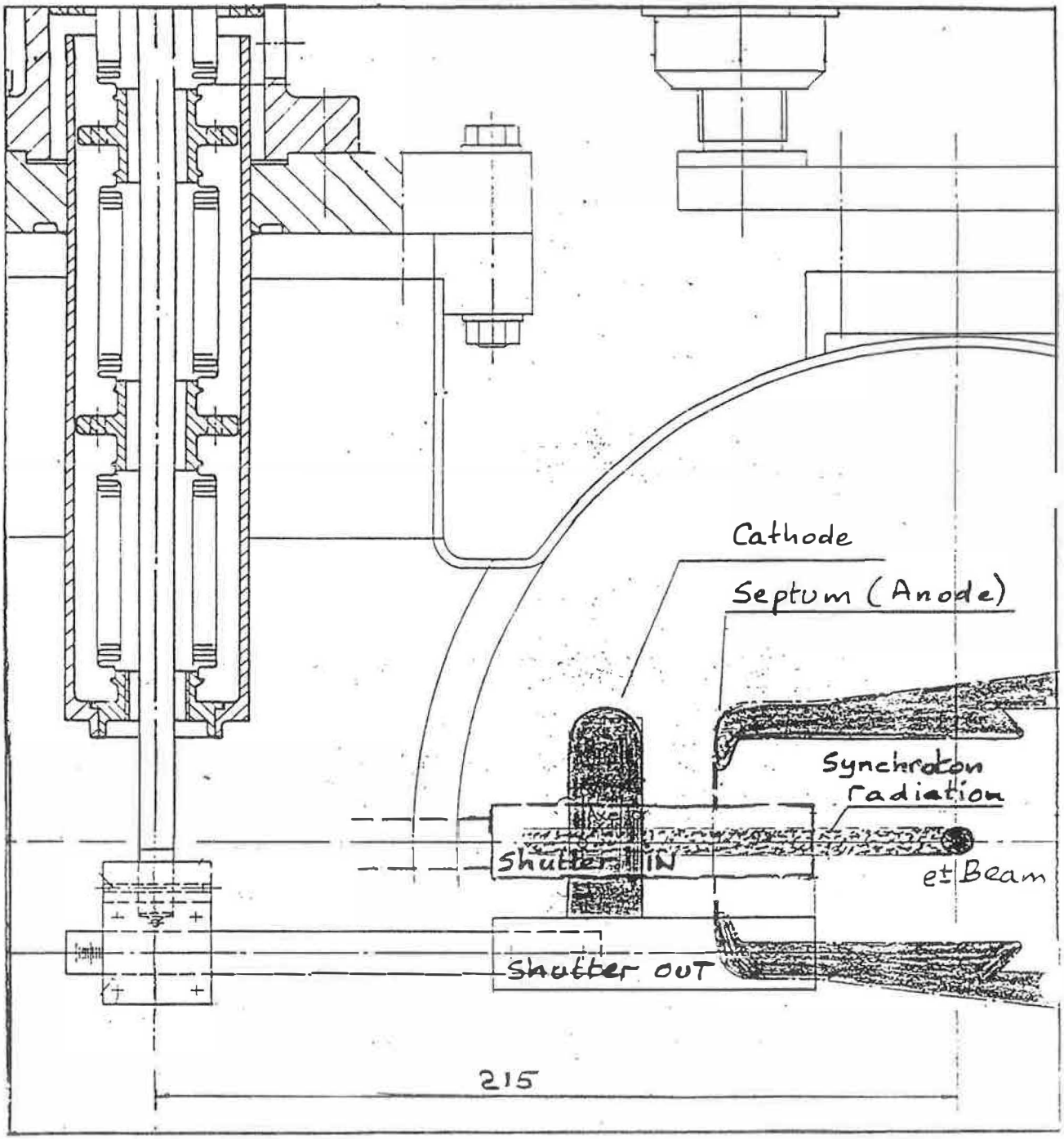

Fig. 1. - Position and displacement of the shutter.

2. ESTIMATION OF THE NUMBER OF PHOTONS RECEIVED BY THE CATHODE AND OF THE PHOTO EMISSION CURRENTS.

The number of photons of mean energy emitted from the circular path of the orbit of the SPS, radius ρ = 741.3 m, is :

$$\overline{n_\gamma}\ [10^{14}\ m^{-1}\ s^{-1}] = 1.73\ E\ [GeV]\ i\ [mA] \qquad (1)$$

where i is the current of the circulating positrons (resp. electrons) and E their energy.

According to Fig. 2, the number of photons of mean energy, received on a surface S in a straight section is :

$$N_\gamma\ [s^{-1}] = \overline{n}_\gamma \int_S \rho\ d\beta \qquad (2)$$

The geometry of the e.s. septum is shown in Fig. 3. The number of photos received by the various cathodes may be calculated assuming that the anode is transparent for the incoming photons. This is not entirely true because the tungsten wires are 0.1 mm thick and spaced at 1.5 mm. The calculated numbers are given in Table 1 :

- Line 1 : $n_\gamma = N_\gamma / E * i$, the number of photons received per second, GeV and mA.
- Line 2 the number of photons N_γ per second for the maximum positron energy of 20 GeV and the nominal positron current i of 0.45 mA (8 bunches of $8 * 10^9$ positrons each).

For estimating the current I of photo-electrons emitted from the cathode, the following relation is used :

$$I = N_\gamma\ \delta\ e\ /\ \sin\alpha \qquad (3)$$

where $e = 1.6 * 10^{-19}$ A s, δ is the coefficient for the emission of photo electrons and α the angle of incident photons.

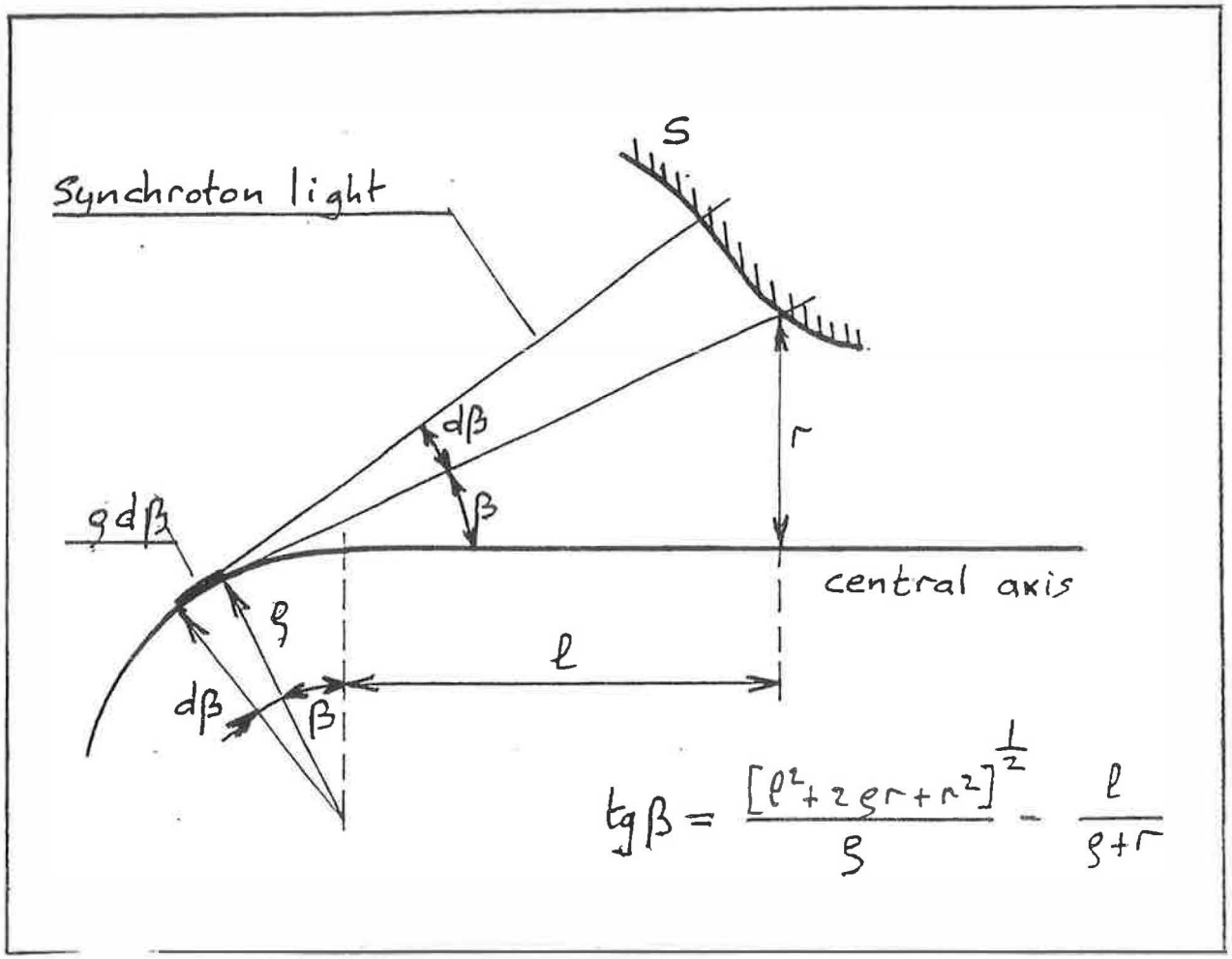

Fig. 2. - Geometry of synchroton light emission.

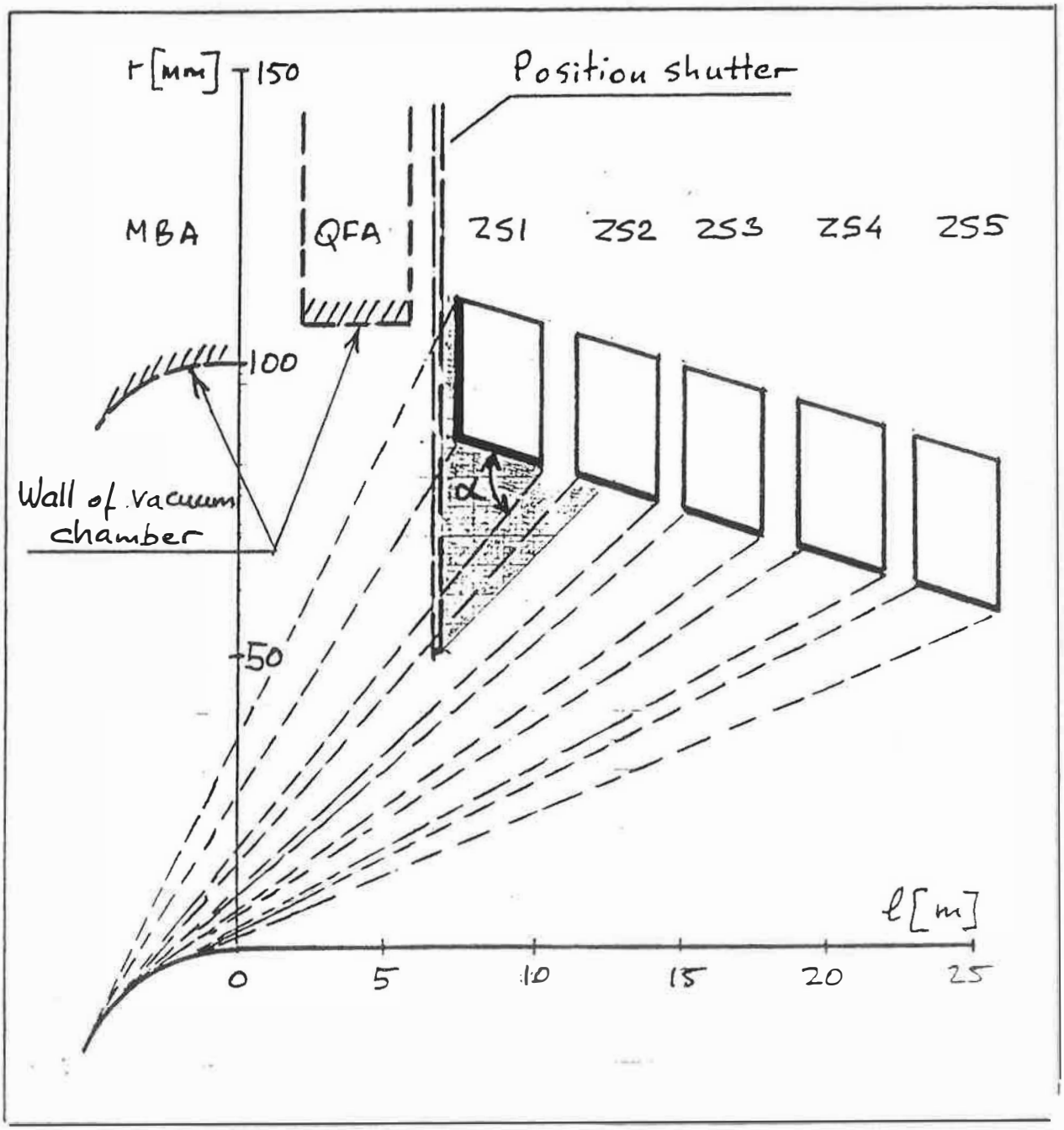

Fig. 3. - Geometry of the electrostatic septa neglecting the septum wires and the shadow cast by the shutter.

P A R A M E T E R	ZS1		ZS2	ZS3	ZS4	ZS5	Total
	Front	Side	Side	Side	Side	Side	ZS
n_γ [10^{-14} s^{-1} GeV^{-1} mA^{-1}]	5.4	2.2	2.2	1.4	1.0	0.8	13.0
N_γ [10^{-14} s^{-1}] for E = 20 GeV, i = .45 mA	48.	20.	20.	13.	9.	7.	117.
i_S [μA GeV^{-1} mA^{-1}]	0.4	1.6	1.6	1.3	1.2	1.0	7.1
I [μA] for E = 20 GeV, i = .45 mA	3.9	14.4	14.8	12.0	10.5	9.0	64.6

Table 1. - Number of photons received and photo currents emitted by the individual cathodes.

The specific current $i_s = I/E.i$ and the total current I, lines 3 and 4 of Table 1, have been calculated with $\delta = 4 * 10^{-4}$ which is true for small α. For $\alpha \approx \pi/2$, which is the case at the front face of the septa, the value of σ is assumed to increase 10-fold.

The percentage of the total number of photons received by each cathode is shown graphically in Fig. 4. The front face, which is only 25 mm wide, receives as much as 41% of the total photon flux. The photocurrent, on the contrary, is small because of the overwhelming influence of the sine function in equation (3) which reaches a maximum at $\pi/2$.

The total number of photons received and the total charge liberated during a particular acceleration cycle can be obtained by integration. A typical example showing the evolution of the positron current and energy during the cycle is depicted in Fig. 5.

The total number of photons then is :

$$N_{tot}\ [10^{14}] = \int_{t_{injection}}^{t_{extraction}} n_\gamma\ E(t)\ [GeV]\ i(t)\ [mA]\ dt\ , \qquad (4)$$

where n_γ is given in the first line of Table 1. The total charge will then be :

$$Q_{tot}\ [\mu C] = \int_{t_{injection}}^{t_{extraction}} i_s\ [\mu A\ GeV^{-1}\ mA^{-1}]\ E(t)\ [GeV]\ i(t)\ [mA]\ dt \qquad (5)$$

where i_s is given in the third line of Table 1.

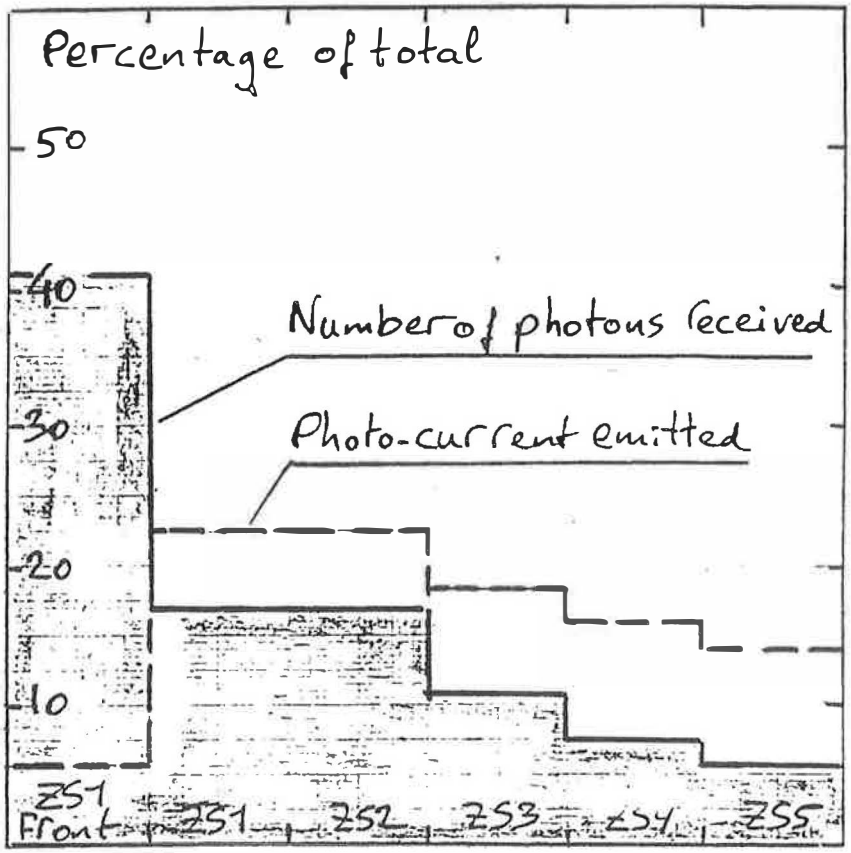

Fig. 4. - Estimated number of photons and photo-current for each cathode.

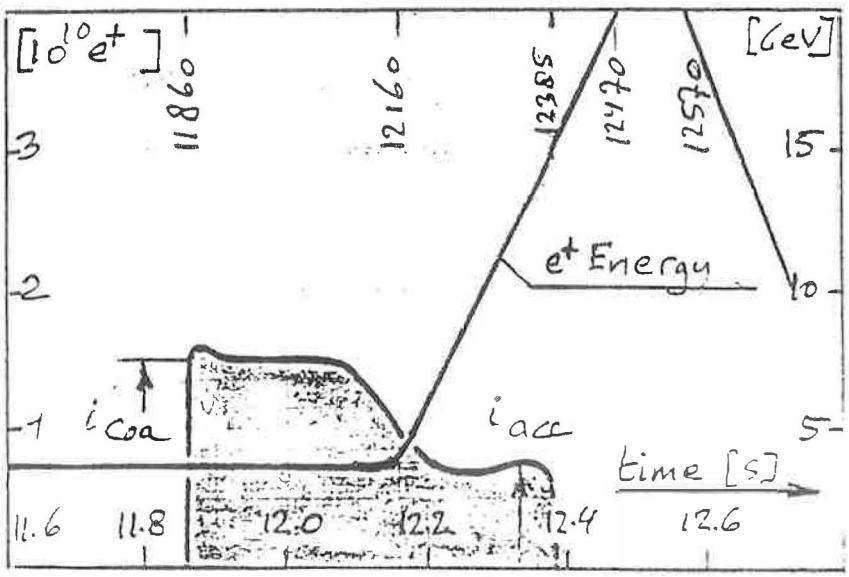

Fig. 5. - Observed positron intensity during the acceleration cycle.

The actual charge liberated may be approximated by plugging-in some real parameters. Noting that, see Fig. 5., the circulating beam intensity consists of :

- a coasting intensity i_{coa} at 3.5 GeV lasting roughly 310 ms,
- an accelerated intensity i_{acc} where, during a period of time lasting 215 ms, the energy is raised from 3.5 to 16 GeV, equation (5) may now be transformed to :

$$Q_{tot}\ [\mu c] = 7.1\ [3.5 * 0.310 * i_{coa} + i_{acc} \int_0^{0.215} E\ dt]$$

$$E = 3.5 + \frac{t}{0.215}\ (16 - 3.5)$$

$$Q_{tot}\ [\mu c] = 7.1\ [1.1\ i_{coa} + 2.1\ i_{acc}] \qquad (6)$$

The relation between the number of circulating positrons N_{e^+} and the circulating beam current is :

$$i\ [mA] = 6.94\ 10^{-12}\ N_{e^+} \qquad (7)$$

The effective beam intensity is then defined as :

$$i_{eff}\ [mA] = 1.1 * i_{coa}\ [mA] + 2.1 * i_{acc}\ [mA] \qquad (8)$$

3. PHOTON EMISSION CURRENTS MEASURED.

3.1. The HT-circuit.

The HT-circuit of the e.s septa, shown in Fig. 6., is such that only the sum of the photo currents I_{tot} could be measured eventually. Because the RC time constant of the circuit is of the order of 20 s the only parameter which can be extracted reliably is the charge Q_{tot}, as defined by equation (5). The magnitude is evaluated by integrating the power supply current registered by a recording instrument.

The individual anode currents I_{ai} between anode and earth have been measured with low accuracy. If there were no secondary effects, the total emitted charge should be equal to the received charge, or :

$$Q_{tot} = \sum_{i=1}^{5} I_{ai}\, dt \qquad (9)$$

It turns out that this is not the case.

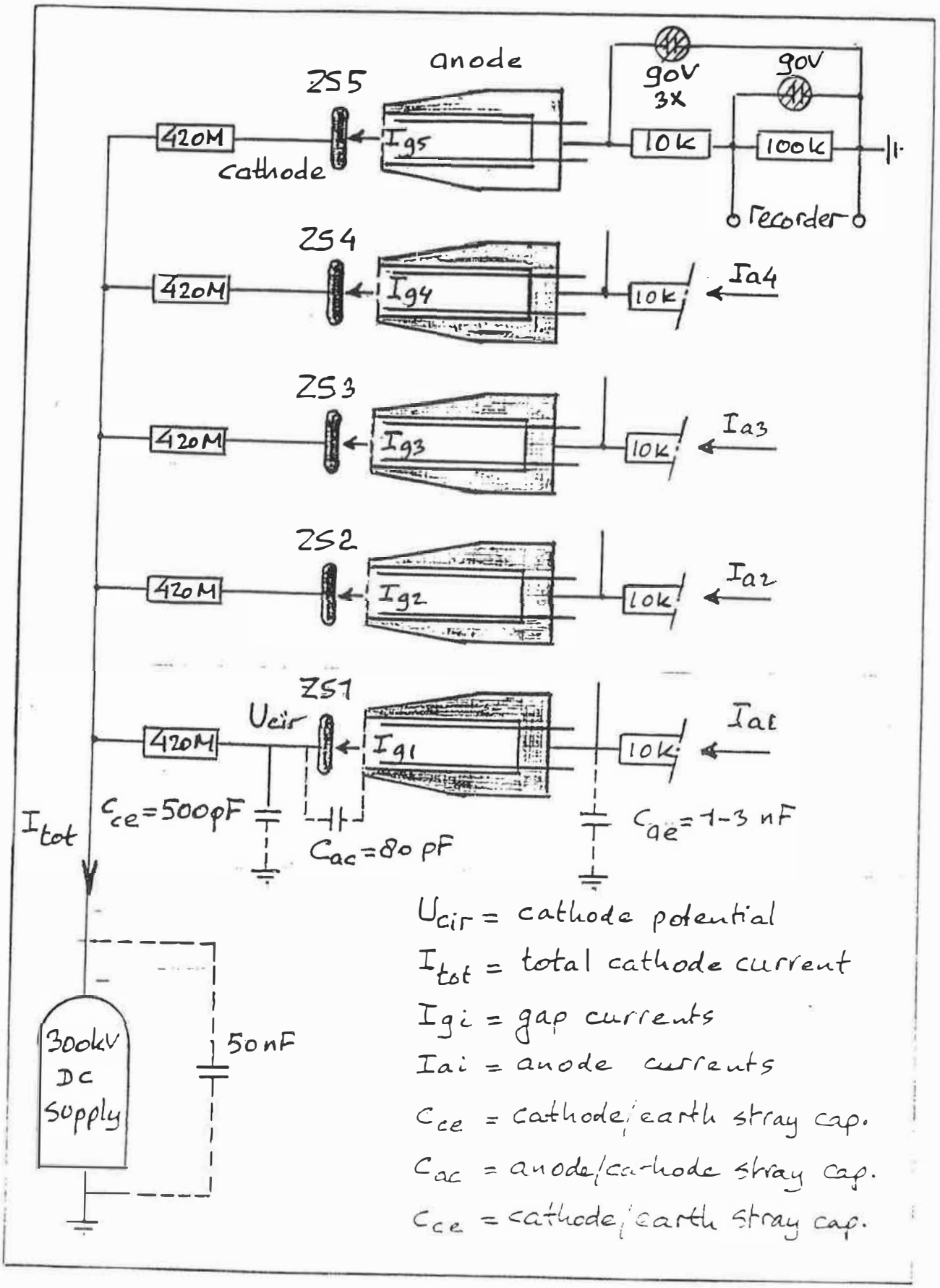

Fig. 6. - The HT-circuit of the e.s septa.

3.2. Photo emission currents at constant cathode potential.

The total cathode current caused by photo emission I_{tot} and the individual anode currents I_{ai} have been recorded at constant cathode potential, U_{cir} = 200 kV, in the latter case with and without shutter. The graphs, without shutter are shown in Fig. 7.

The following remarks are relevant :

- The circulating number of e^+, E ≈ 16 GeV, was of the order of $2 * 10^{10}$. No calibration was available.

- The polarity of the currents corresponds with the emission of photo-electrons from the cathode.

- The sum of the anode currents is much less than the cathode current. Equation (9) is therefore strongly violated, most likely because the wire septa are transparent to 200 keV electrons.

- The total cathode charge predicted by equation (6) is of the order of 3 μc which is of the order of what has been measured, namely 5.6 μc.

- Activating the shutter reduces the cathode charge to 0.7 μc and $I_{a1} = I_{a2} = I_{a3} = 0$ showing that some 90% of the total anode current is produced by the first ZS.

- The current profile observed along the extraction channel does not agree with Fig. 4. which predicts nearly equal currents in ZS1 and ZS2 and a very gentle drop downstream.

- A possible explication is based on the presence of the array of septum wires, shown in Fig. 8., which act as a screen, especially for the downstream septa where the synchroton light has incident angles of a few mrad only and the light has to traverse or is scattered by some 20 wires.

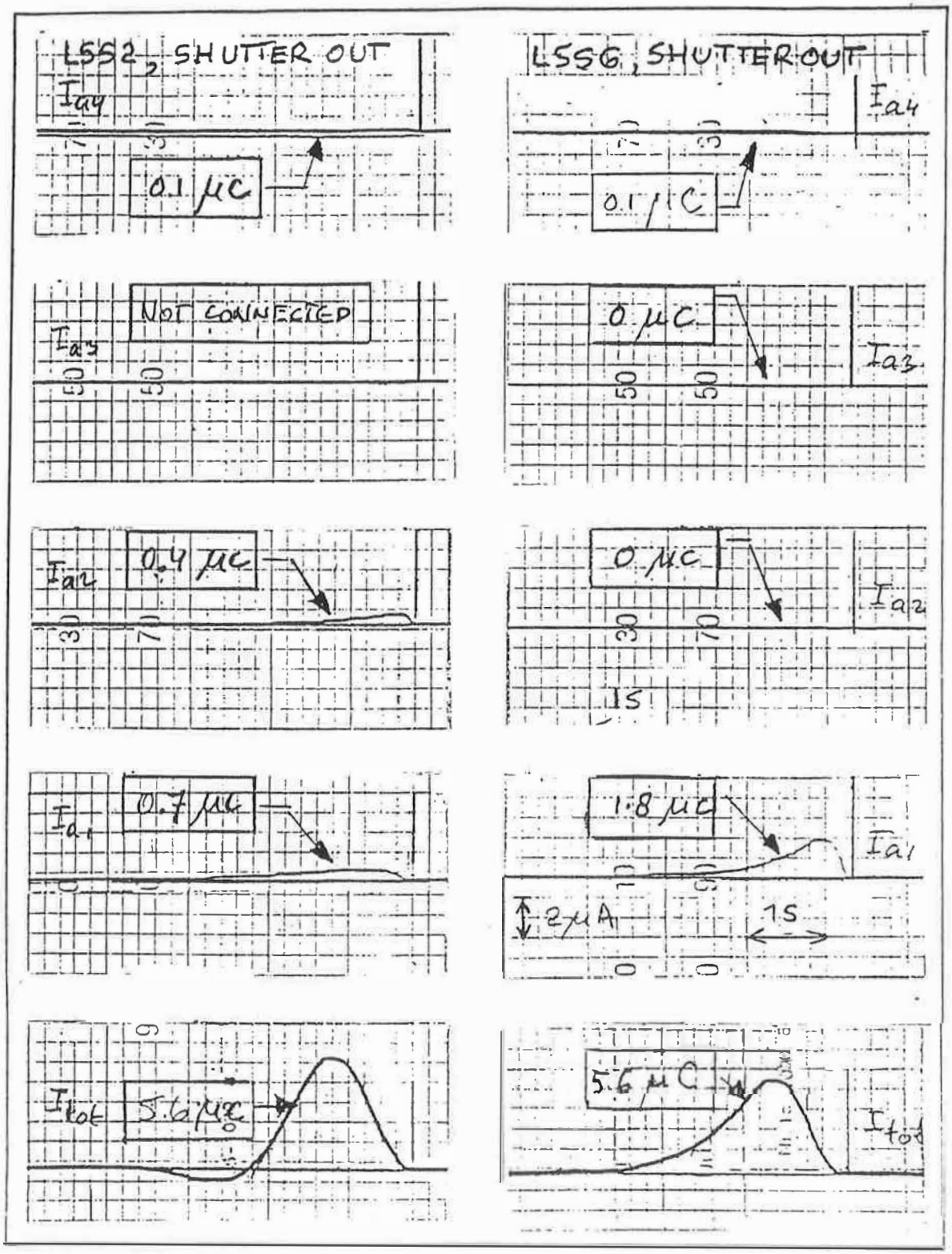

Fig. 7. - Photo emission currents in LSS2 and LSS6 with shutter out.

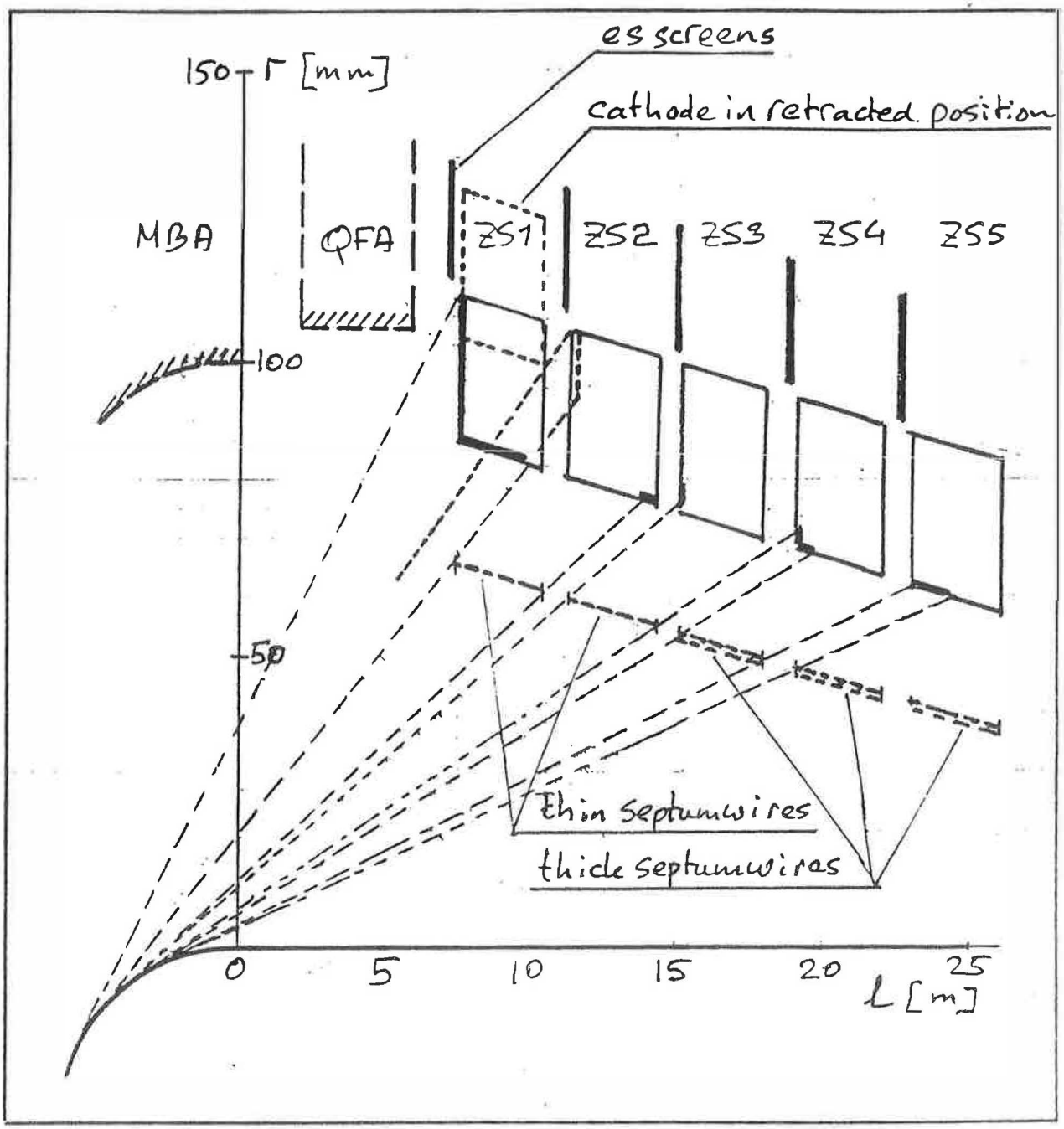

Fig. 8. - Geometry of the electrostatic septa with septum wires and the position of the retracted cathode.

A preliminary attempt has been made to relate the measured liberated charge Q_{tot} and the effective beam intensity as defined by equation (8). The resulting graph is shown in Fig. 9. :

- The graph would reveal a non-linear effect. For small effective circulating beam intensities, less charge would be emitted.

- This effect has to be confirmed by improved measurements where the charge and effective currents are evaluated in real time using a computer program.

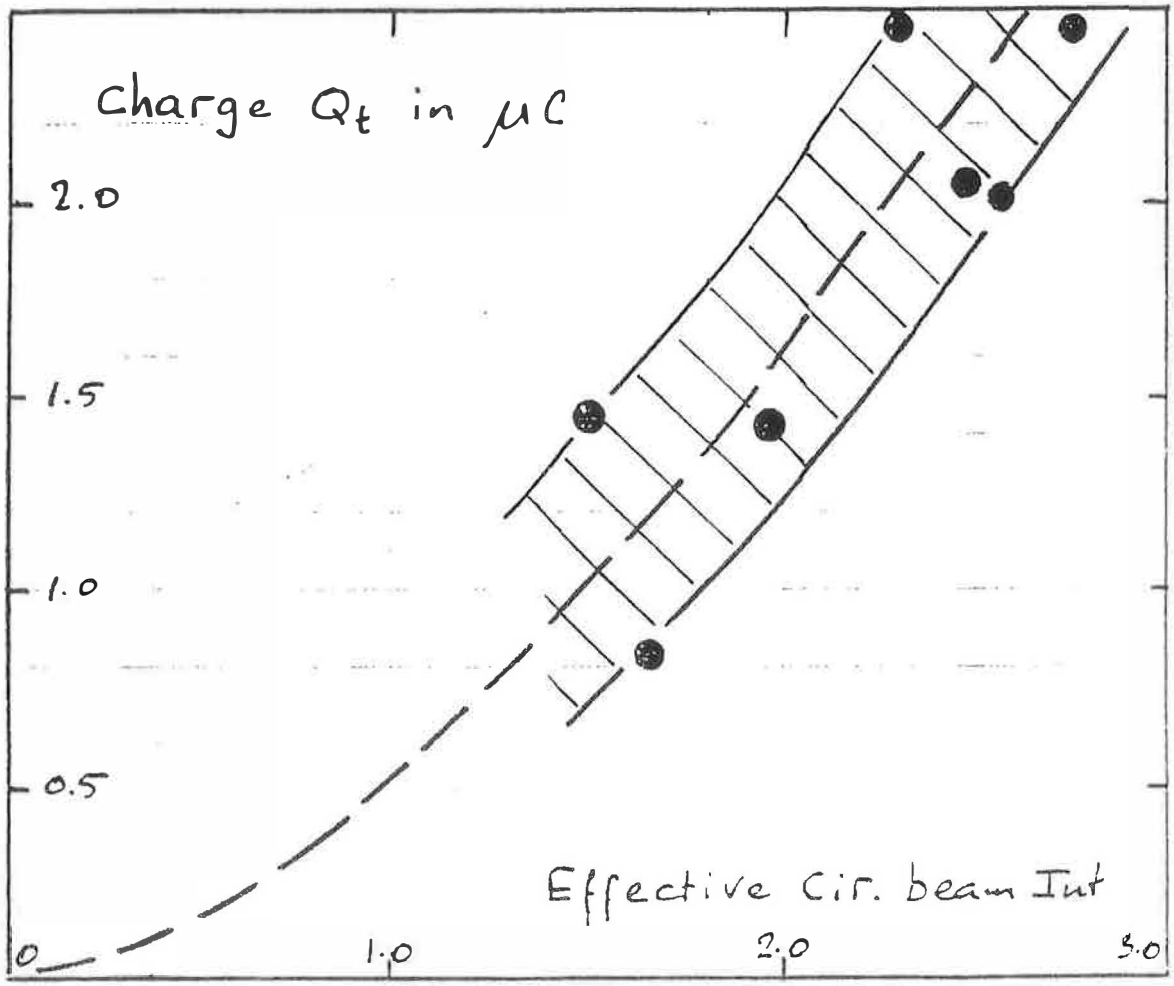

Fig. 9. - The charge emitted by the cathode as function of the circulating beam intensity (in arbitrary units).

A second study was undertaken to investigate the dependence of the emitted charge and circulating beam intensity at various cathode voltages.

The results suggest the following :

- The emitted cathode charge increases with cathode potential.
- At 10 kV, there is already a considerable photo-electric charge flowing.
- Saturation sets-in at 100 kV.
- For pulsed HT, in order to reduce anode currents and related sparks, it would be necessary to discharge the circuit completely.
- No graph is shown because the preliminary results are not very precise.

4. SPARKING OF THE SEPTA.

4.1. Spark time spectra and shutter efficiency.

Spark time spectra have been measured during simultaneous p and e^+-operation and during e^+-operation. Only the conclusions in both cases are identical, with the difference that during simultaneous operation a p-induced spark background is created which partially masks the so called retarded sparks.

The spark time spectra during e^+-operation are shown in Fig. 10. The left figure (LSS2) shows that, with the shutter in position "OUT", very strong peaks are present in ZS1, ZS2 and ZS4. One septum, ZS3, was not connected at that time. The right figure (LSS6) shows what happens when the shutter is in position "IN". The peak around 12 s has disappeared in ZS1 and ZS2. A strong peak is still visible in ZS3 and ZS4 was not connected.

The following remarks are relevant :

- Around cycle time 12 s, there is a characteristic prompt spark peak with a very short decay time.

- The background consists of retarded sparks caused by e^+ operation.

- The available information indicates that both extraction channels behave similarly.

- The lefthanded figure shows strong sparking in ZS2 because the interelectrode gap of ZS1 was set at 39 mm instead of the customary 20 mm. The reason for this will be explained later. However, it has been shown with all gaps set at 20 mm that for both kinds of operation, e^+p and e^+, ZS2 does not seem to produce prompt sparks.

- ZS5 also never features the prompt sparking peak.

- The shutter eliminates, under the given conditions of 2 × 10^{10} e^+pp and up to 16 GeV, all sparking in ZS1.

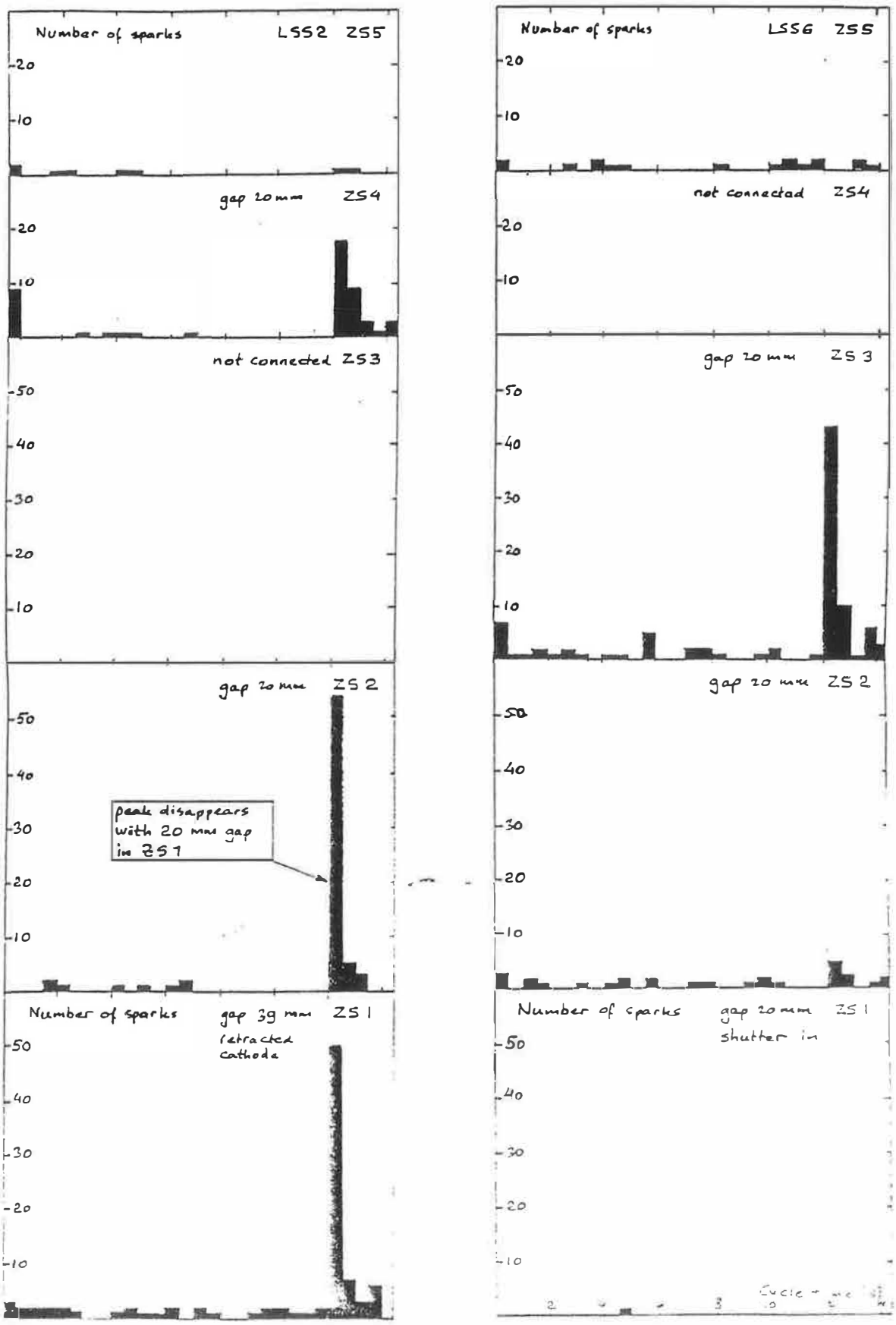

Fig. 10. - The spark time spectra with shutter in position "OUT" (left) and "IN" (right).

4.2. Spark rate decay time constants of prompt and retarded sparking.

The decay time constant of prompt sparking.

The spectrum of prompt sparks from 11.860 s to nearly the end of the cycle at 14.400 s is shown in Fig. 11. The following points are important.

- The injection of positrons around 11.860 s does not lead immediately to sparking.
- Sparking sets in around 12.100 s prior to acceleration which takes place at 12.170 s.
- Hereafter, the spark rate rises more or less linearly with energy and reaches a maximum between 12.368 and 12.385 s exactly at the instant the beam is lost.
- The spark rate then decays with a time constant of 50 ms.
- After 200 ms, follows a long tail of retarded sparks with a decay time constant of 6 s.
- It is not clear at this stage at what instant the retarded spark spectrum starts, whether the two peaks are superposed (i.e. two spark triggering mechanisms), or whether they follow each other (i.e. only one mechanism).

The decay time constant of retarded sparks.

The spectrum of retarded sparks, Fig. 12., consists of all the sparks produced in LSS2 and LSS6 to improve the statistics. Thus, it becomes clear that the prompt spark peak is followed by a long tail of sparks which are triggered as much as 15 s after the main event.

- The tail can be fitted with an exponential having a time constant $\tau_r = 6$ s.
- Similar observations have been made during mixed e^+p-operation.

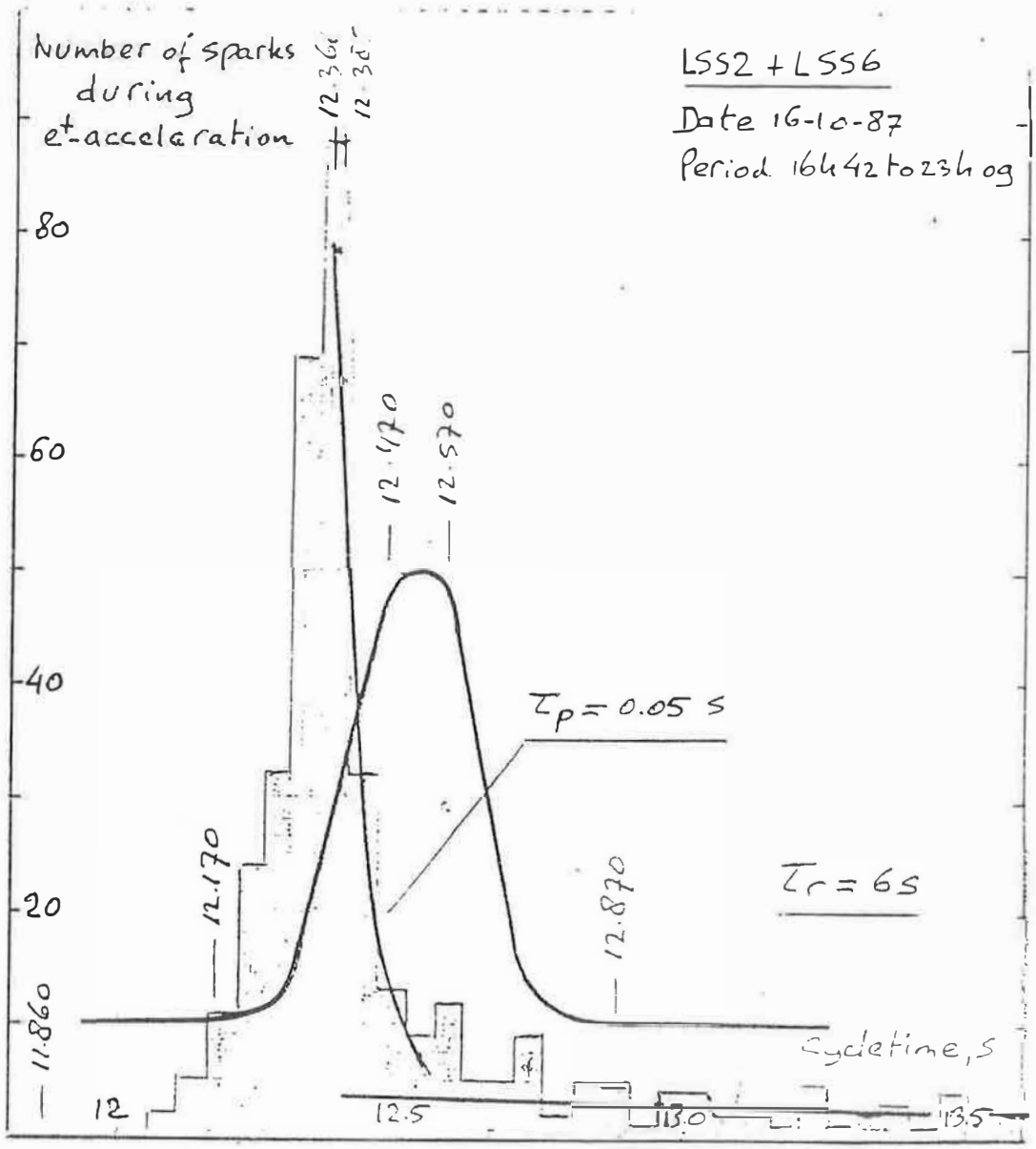

Fig. 11. - Spectrum of the prompt sparks.

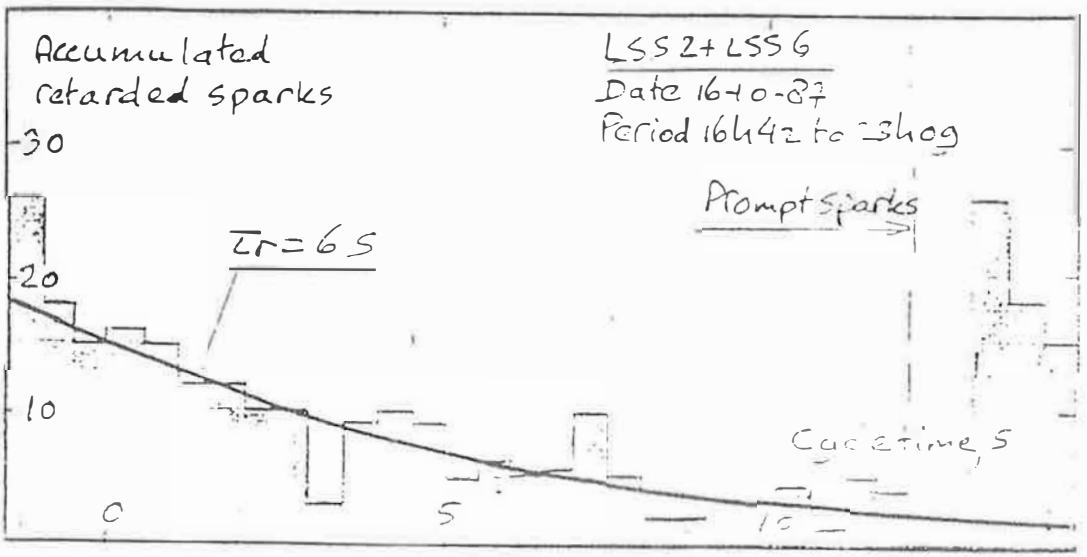

Fig. 12. - Spectrum of the retarded sparks.

- Such a long time constant suggests a thermal process involving the septum wires.

- Calculations show that indeed the expected time constant of the wires ($\tau_r \approx 7$ s) agrees with the observed value of the decay rate ($\tau_r \approx 6$ s).

- The very rapid decline of the prompt spark rate cannot be explained by the computer simulation and one therefore has to conclude that the spark spectrum consists of two independent contributions the prompt sparks and the retarded sparks.

- The fact that the prompt to retarded spark ratio of a given septum varies considerably with time supports the hypothesis of 2 different mechanisms.

Prompt and retarded spark distributions along the extraction channels.

The spark distributions along the LSS6 extraction channel, with or without shutter, have been analysed and are shown in Figs. 13. and 14.

- Without shutter, roughly 80% of the sparks are produced by ZS1 ; hardly any sparks are produced by ZS2 ; the spark rate rises slowly in ZS3 and ZS4 ; in ZS5 the spark rate diminishes strongly.

- The shutter eliminates all sparking in ZS1 but causes higher spark rates in ZS2, ZS3 (ZS4 not connected) and ZS5.

- The shutter therefore might act as a scatterer for synchroton light.

- As will be demonstrated later, the prompt sparks are probably triggered by the front end of the cathodes which explains the strong peak of the prompt sparks in ZS1. Because anodized Al_2O_3 is very porous, a total absorption of the photons could cause very strong local outgassing or even sputtering.

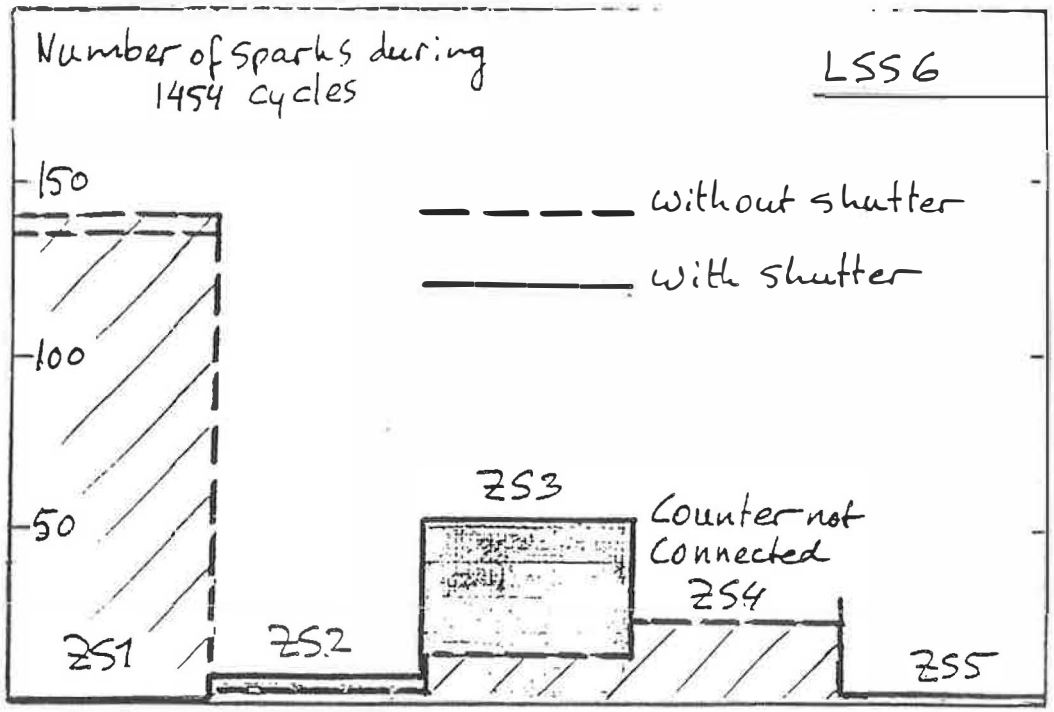

Fig. 13. - The prompt spark distribution along the extraction the extraction channel with and without shutter.

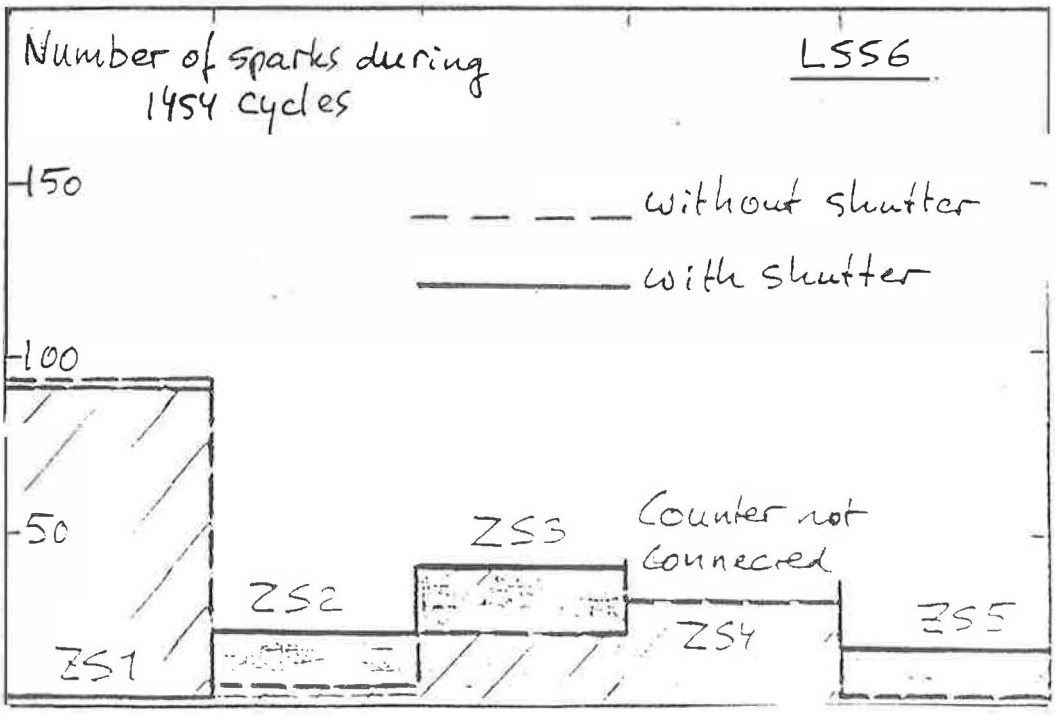

Fig. 14. - The retarded spark distribution along the extraction channel with and without shutter.

- Fig. 8. shows that the front end of the cathodes of ZS2 and ZS5 are shielded by the septum wires and that ZS3 and ZS4 are not, which would explain the presence of prompt sparks in the latter two septa (see Fig. 10).

- The retarded sparks then could be caused by the septum wires which then would cause sparking by local outgassing. The wires in ZS2 are strongly outgassed by p-extraction which could explain the low spark rate in the second septum.

- There remains the problem to understand the high spark rate of retarded sparks in ZS1 which should be low because the septum wires are perfectly outgassed by the ρ-losses. The key to the problem may again be found in Fig. 8. which shows that the side of the cathode is illuminated over its entire length by photons giving rise to a third mechanism which also seems to have a long time constant.
  It could also be that the front end of the cathode causes both prompt and retarded sparks.

4.3. The retracted cathode experiment.

In order to test the sensitivity of the upstream cathode ends to synchroton light, it was decided to measure the spark rates with the anode gap in ZS1 set at 20 mm and 39 mm. Fig. 8. shows that in the latter case the front end of ZS2 is exposed to the photon flux. The resulting spark spectrum is shown in Fig. 10. (left hand figure), Figs. 15. and 16. The following remarks can be made :

- With a 20 mm gap, virtually, no sparks are produced in ZS2, with a 39 mm gap both the prompt and retarded spark rates increase dramatically.

- With a 20 mm gap, 85% of the prompt sparks, Fig. 15., are produced in ZS1 and none in ZS2, with a 39 mm gap the prompt sparks are evenly divided between ZS1 and ZS2.

- The percentage of sparks in ZS4 and ZS5 remains unchanged.

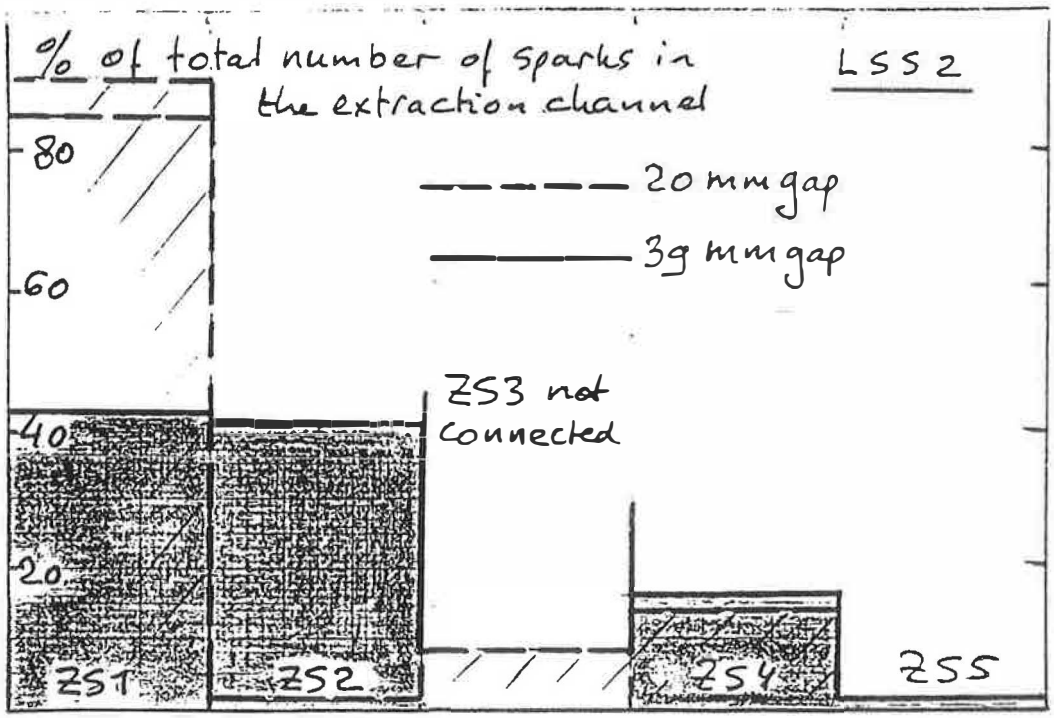

Fig. 15. - The prompt spark distribution along the extraction channel with 20 and 39 mm gaps in ZS1.

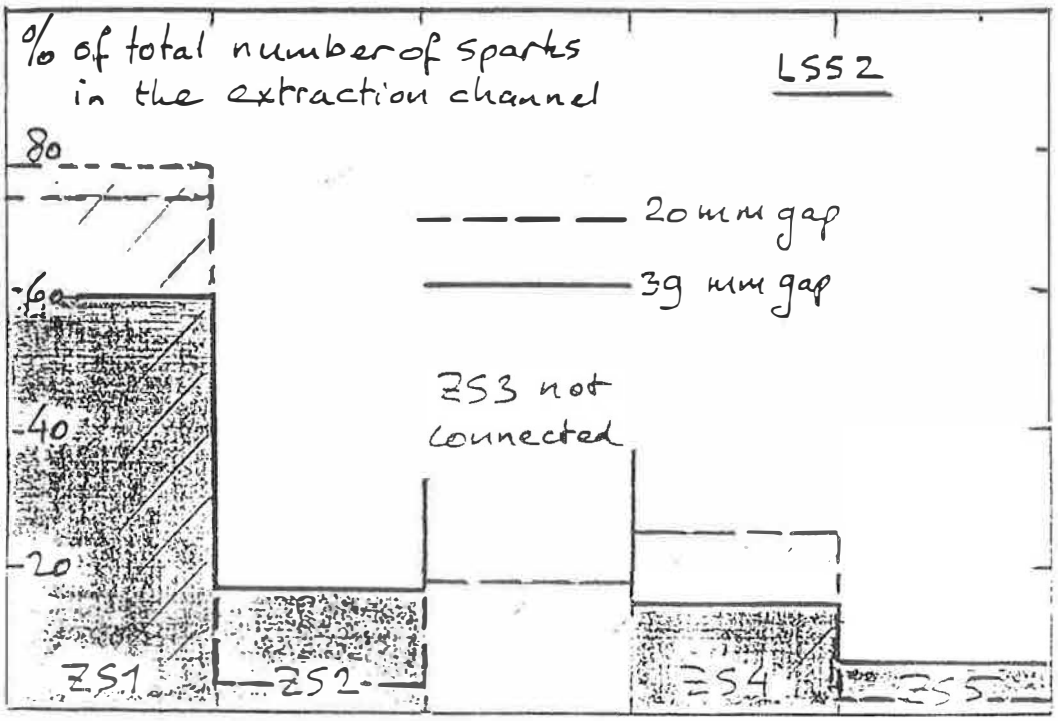

Fig. 16. - The retarded spark distribution along the extraction channel with 20 and 39 mm gaps in ZS1.

- This behaviour would signify that the prompt sparks in ZS1 and ZS2 are caused by the exposure of the front end of the cathodes to synchroton light.

- ZS1 sparks less because of the e.s screen mounted in front of the cathode (see Fig. 8.).

- With a 20 mm gap, 80% of the retarded sparks are produced in ZS1, see Fig. 16. With a 39 mm gap, the spark rate in ZS1 diminishes somewhat but still peaks in forward direction. The spark rate in ZS2 increases strongly.

- This then would mean that the front ends produce both prompt and retarded sparks.

- It would be interesting to perform the retracted cathode experiment with ZS2, ZS3 and ZS4.

5. CONCLUSIONS.

The interaction of synchroton radiation with the e.s septa may be summarized by the following statements :

- The photo currents emitted by the cathodes are of the order as predicted. However, the low value of the anode currents can only be understood if wire septa are transparent to 200 keV electrons and part of the charge leaks away through the iontraps.

- The steep drop-off of the photo emission current distribution along the extraction channel can only be understood if the septum wires act as a screen for the photons.

- Prompt sparks are apparently caused by the direct interaction of synchroton light with the upstream end of the cathodes. The fast decay of the spark rate could be due to sparking between cathode and the solid metal screen upstream of each septum.

- Retarded sparks are caused by interaction of synchroton light with the cathode or septum wires. A discharge current then develops between the cathode and a septum wire which, once heated by a spark, cools down very slowly giving rise to delayed sparking.

- The second septum never sparks promptly because of screening by the septum wires of ZS1. The retarded spark rate is also very much below average. This could be because the septum wires are perfectly conditioned by previous p-operation.

The performance of the shutter may be summarized as follows :

- The shutter eliminates all sparking in the septum which follows the shutter. The spark rate in the septa more downstream seems to increase slightly.

6. RECOMMENDATIONS.

- All the measurements should be repeated under much more stable conditions.

- The number of photons generated during a cycle should be evaluated for each cycle.

- The circulating beam intensity and energy must be known during each cycle.

- Repeat retracted cathode experiment with ZS2, ZS3 and ZS4, using small displacements to see in which position the following septum starts sparking.

- ZS1 and ZS2 have thin septum wires and the other septa have thick wires, measure a possible difference in retarded spark behaviour.

- Repeat spark rate experiments with several cathode potentials.

7. ACKNOWLEDGEMENTS.

S. SCHALK prepared all the electronics in LSS2 and LSS6 for the measurements and M. GYR calculated the thermal time constants of the septum wires for which the authors are very grateful.